White Light Dispersion Measurements by One- and Two-Dimensional Spectral Interference

D. Meshulach, D. Yelin, and Y. Silberberg

***Abstract*— White light dispersion measurements by one- and two-dimensional spectral interference are shown. One-dimensional white light spectral interference measurements allow accurate characterization of dispersion using weak optical fields. Two-dimensional spectral interference allows for real-time measurements since no post-processing is needed, and therefore can be used in situations where the optical properties of the elements under test vary in time. We demonstrate the applicability of the two methods for characterizing dispersive elements such as optical glasses and dielectric coatings.**

***Index Terms*—Dispersion measurements, group velocity dispersion, spectral interference, white light.**

I. Introduction

DISPERSION phenomena has constantly presented limitations on the generation, manipulation, and measurement of ultrashort optical pulses. Passively mode-locked solid-state femtosecond lasers generally operate in a dispersion-limited regime, and precise knowledge and control over the intracavity dispersion is essential for stable operation [1]. Almost any application of ultrashort pulses requires precise knowledge of the phase relations between the optical components of the pulse which are introduced by various optical elements in the system. For example, in optical pulse compression, tailored dispersive elements are used to accomplish efficient compression [2]. Techniques for characterization of optical pulses involve the use of optical components such as beam splitters and mirrors, which contribute to the total dispersion of the system, and consequently affect the measurement. Dispersion characterization of such components is therefore required in order to account for its effect.

One of the most common techniques for measuring dispersion of optical components was investigated in the late 1800's by Michelson [3] and is now referred to as white light Fringe Contour Shift (FCS) [4], [5]. This white light interferometric technique involves measurements of the interference signal of a filtered white light beam which emerges from a Michelson interferometer, in which the dispersive element under test has been placed in the path of the signal beam. For different wavelengths, the relative delay between the two arms of the interferometer changes. The group velocity dispersion of the unknown element is obtained by plotting the delay of the peak of the interference fringes envelope as a function of wavelength. A variation of this technique has been used successfully for dispersion measurements of single-mode optical fibers [6], [7]. In situations where the reflectance or transmittance of the dispersive element varies significantly over the bandwidth of the filtered light, or when the variation of the group delay dispersion is comparable to the coherence time of the filtered light, the envelope of the fringes is not well defined, and the FCS technique fails. In such situations, the technique of phase-locked interferometry (PLI) is often used, in which a feedback loop locks the interferometer to a single fringe. In PLI, as in FCS, the group velocity dispersion is obtained by plotting the change in the reference arm length as the filter is scanned over the entire bandwidth of the source [8], [9].

Recently, a measurement of ultraweak ultrashort pulses was demonstrated using a one-dimensional (1-D) spectral interference (SI) technique [10], introduced by Froehly *et al.* [11]–[13]. This technique involves a linear measurement of the spectral interference of two pulses, delayed in time by τ with respect to each other. The measurement yields the spectral phase difference $\phi_{\rm sig}(\omega) - \phi_{\rm ref}(\omega) - \omega\tau$, where $\phi_{\rm sig}(\omega)$ and $\phi_{\rm ref}(\omega)$ are the spectral phases of the unknown signal pulse and a characterized reference pulse, respectively. In the case where the signal pulse and reference pulse are derived from the same source and one undergoes a spectral phase distortion, the obtained spectral phase difference between the signal and the reference pulse is simply the dispersion of the element. This principle was used as a basis for a two-dimensional (2-D) spatial-spectral interference (SSI) technique [14]–[16].

In this paper, we demonstrate 1-D and 2-D dispersion measurements by white light SI. The 1-D SI measurement scheme involves the use of a white light source, which replaces the pulsed laser source, used in most previous work [10]–[13]. The 2-D SI measurement scheme, as in the work of [14] and [16], involves the measurement of the 2-D SI between white light reference and signal fields, propagating at an angle with respect to each other. The optical frequencies of the propagating fields are angularly dispersed by a prism and interfere at the focal plane of a cylindrical lens, where a CCD matrix is placed.

The techniques of white light SI and SSI allow for sensitive and accurate determination of dispersion over a large bandwidth. In the method of SI, post-processing is needed to extract the dispersion from the measured data, and unwrapping of the spectral phase is needed, as well as the need to resolve the sign ambiguity of the phase. The method of SSI, as we show, allows real-time determination of dispersion over a large bandwidth, while unwrapping of the spectral phase is not needed. This is most desired in situations which involve

Manuscript received May 9, 1997; revised July 10, 1997.

The authors are with the Department of Physics of Complex Systems, The Weizmann Institute of Science, Rehovot 76100, Israel.

Publisher Item Identifier S 0018-9197(97)07820-2.

dynamic measurements, such as when aligning an optical setup for minimum dispersion. We demonstrate the potential of white light SI and SSI techniques by measuring small and large dispersions of optical glass flats, dielectric mirrors, and prism-pair arrangements.

II. Theory

A. Spectral Interference

One-dimensional white light SI involves the measurement of the power spectrum of the combined field of a reference field and a time delayed signal field. Consider the experimental setup shown in Fig. 1, where a spatially filtered collimated white light beam is split into two arms of a Michelson interferometer and recombined after introducing a time delay into the signal arm. The power spectrum of the combined field of the random reference field $\mathbf{r}(t)$ and the delayed random signal field $\mathbf{s}(t-\tau)$ is given by

$$\begin{aligned} I(\omega) &= |\mathbf{R}(\omega)\exp(i\mathbf{\Phi}_R(\omega)) + \mathbf{S}(\omega)\exp(i\mathbf{\Phi}_S(\omega)) \\ &\quad \times \exp(-i\omega\tau)|^2 \\ &= |\mathbf{R}(\omega)|^2 + |\mathbf{S}(\omega)|^2 + 2|\mathbf{R}(\omega)||\mathbf{S}(\omega)| \\ &\quad \times \cos(\mathbf{\Phi}_S(\omega) - \mathbf{\Phi}_R(\omega) - \omega\tau). \end{aligned} \tag{1}$$

Here $\mathbf{S}(\omega) = \mathbf{R}(\omega)H(\omega)$ and $\mathbf{R}(\omega)$ are the random spectral amplitudes of the signal and reference fields, respectively, with $H(\omega)$ the transfer function of the tested element. The functions $\mathbf{\Phi}_S(\omega)$ and $\mathbf{\Phi}_R(\omega)$ are the corresponding random spectral phases. It is evident from (1) that SI requires that the spectra of the signal field lies within that of the reference field, since spectral interference takes place only between identical spectral components. It is also evident that since the spectral phase difference appears as the argument of the cosine term, unwrapping of the phase is needed, as well as removing of the sign ambiguity. It is important to emphasize that although the phases $\mathbf{\Phi}_S(\omega)$ and $\mathbf{\Phi}_R(\omega)$ are random functions, at any frequency ω, the difference between these two functions remains a constant for a stationary distortion. In particular, when the signal beam undergoes a spectral phase distortion such as dispersion, so that $H(\omega) = \exp[i\Phi(\omega)]$, the argument of the cosine term in (1) is simply the dispersion of the distorting element, up to a linear term, $\Phi(\omega) - \omega\tau$. The delay τ serves as a carrier frequency for encoding of the spectral information. It can be verified that the fringe contrast is maximized when the power spectrum of the two fields are identical. However, this is not a requirement of SI, since spectral phase differences are measured as amplitude modulations of the combined power spectrum.

B. Spatial–Spectral Interference

Consider the geometry of Fig. 2, where a white light reference and signal fields $\mathbf{r}(t)$ and $\mathbf{s}(t)$ are propagating at an angle 2θ with respect to each other and impinging upon a prism. The angle 2θ is controlled by the corner reflector. The prism and the cylindrical lens map the optical frequencies of the two fields at the focal plane of the lens, along the x direction. The field along the perpendicular y direction is not

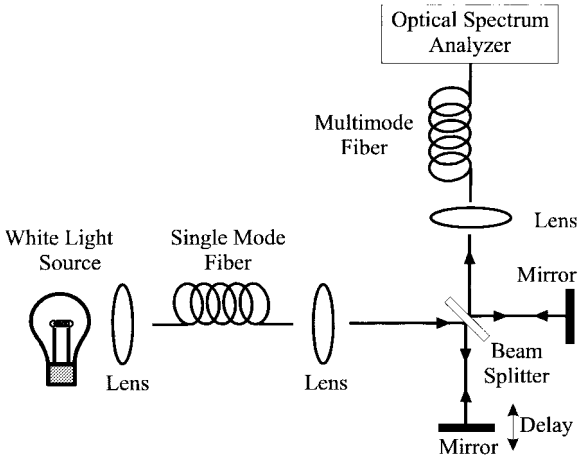

Fig. 1. Experimental arrangement for white light SI measurements.

affected. The 2-D interference intensity, $I(x,y)$, at the focal plane of the cylindrical lens is given by

$$\begin{aligned} I(x,y) &= |\mathbf{R}(x_\omega)\exp(i\mathbf{\Phi}_R(x_\omega))\exp(ik(x_\omega)(f\cos\theta \\ &\quad + y\sin\theta))A(y) + \mathbf{S}(x_\omega)\exp(i\mathbf{\Phi}_S(x_\omega)) \\ &\quad \times \exp(ik_x(f\cos\theta - y\sin\theta))A(y)|^2 \\ &= A^2(y)\{|\mathbf{R}(x_\omega)|^2 + |\mathbf{S}(x_\omega)|^2 + 2|\mathbf{R}(x_\omega)||\mathbf{S}(x_\omega)| \\ &\quad \times \cos(\mathbf{\Phi}_S(x_\omega) - \mathbf{\Phi}_R(x_\omega) - 2k(x_\omega)y\sin\theta)\}. \end{aligned} \tag{2}$$

Here $\mathbf{S}(x_\omega) = \mathbf{R}(x_\omega)H(x_\omega)$, where $\mathbf{S}(x_\omega)$ and $\mathbf{R}(x_\omega)$ are the random spectral amplitudes of the signal and the reference fields, respectively, mapped onto the x direction, and $H(x_\omega)$ is the transfer function of the tested element. The functions $\mathbf{\Phi}_S(x_\omega)$ and $\mathbf{\Phi}_R(x_\omega)$ are the corresponding random spectral phases, and $k(x_\omega)$ is the wavevector magnitude. The subscript ω is included to emphasize the mapping of the optical frequencies onto the x axis. The focal length of the cylindrical lens is f, and $A(y)$ accounts for the intensity distribution in the y direction at the focal plane, assumed to be identical for both fields.

As in SI, although the phases $\mathbf{\Phi}_R(x_\omega)$ and $\mathbf{\Phi}_S(x_\omega)$ are random functions, the difference between these two functions at any frequency remains a constant for a stationary distortion. Therefore, at any x_ω location, the modulation along the y direction has a sinusoidal pattern, shifted by the spectral phase difference between the relevant frequency components. Consequently, any of the fringes traces the spectral phase difference between the two fields as a function of the frequency. The sign ambiguity of the phase difference is removed, and no unwrapping of the phase is needed. Furthermore, the interference pattern provides a natural phase scale, since the fringe spacing along y, for any frequency at location x_ω, corresponds to a 2π phase shift. As in SI, the fringe contrast is maximized when the power spectrum of the fields are equal. However, this is not a requirement of SSI, since as in SI, phase differences are measured as amplitude modulations of the combined power spectrum.

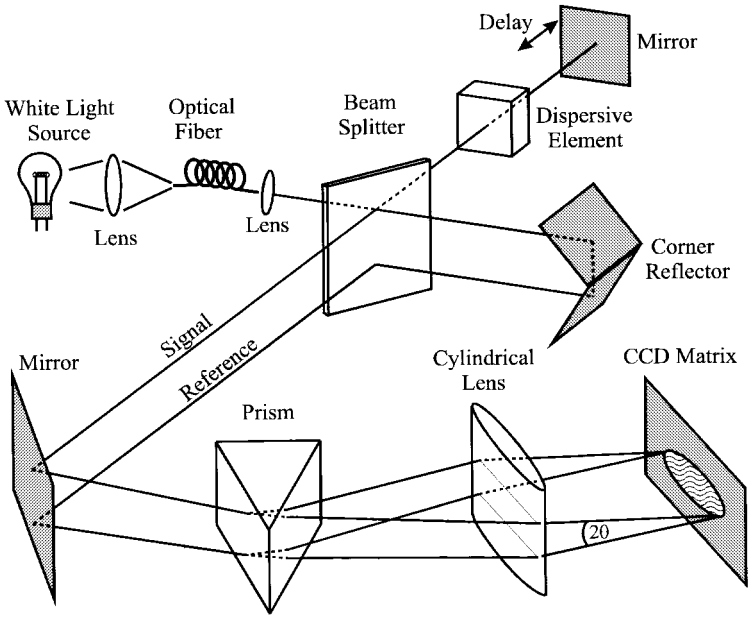

Fig. 2. Experimental arrangement for white light SSI measurements. The reference and the signal fields propagate at an angle 2θ with respect to each other. A color CCD matrix is placed at the focal plane of the cylindrical lens where the spectra of the two fields interfere.

III. Experimental Results

A. Spectral Interference

The SI experimental setup is shown in Fig. 1. The white light source for our experiment was a 250-W Quartz Tungsten Halogen lamp. The light from the lamp was coupled, using a 50-mm focal length lens, into a 5-m-long single-mode optical fiber (at 800 nm), which served as a spatial filter. The light emerging from the optical fiber was collimated using a $\times 10$ 0.25 NA microscope objective. The collimated white light beam was split into two by a broad-band 50/50 dielectric beam splitter (NRC 30B10-BS1). One beam served for the reference field and the other for the signal field. Since the reflecting dielectric layers of the beam splitter were deposited on one side of the beam splitter, the signal beam in our setup passed three times through the beam splitter substrate (BK-7), while the reference beam passed only once. Therefore, a calibration measurement was needed to allow for compensation for this material dispersion in subsequent measurements. The two beams, after having passed again through the beam splitter, were recombined and coupled into a multimode optical fiber, using an additional $\times 10$ 0.25 NA microscope objective. The spectrum of the light emerging from this fiber was measured using an optical spectrum analyzer. All of our data was obtained by integrating over few scans of the spectrum analyzer, to improve the S/N ratio of the measurements. In the following. we describe measurements of phase dispersions that were imposed upon the signal field.

To demonstrate dispersion measurements of optical materials, we first inserted one piece of 0.375-in-thick fused silica glass optical flat in the signal arm of the interferometer. The SI of the combined field, and the smoothed power spectrum of the individual fields is shown in Fig. 3. In order to extract the spectral phase, we smoothed the power spectrum of the reference and the power spectrum of the signal fields and

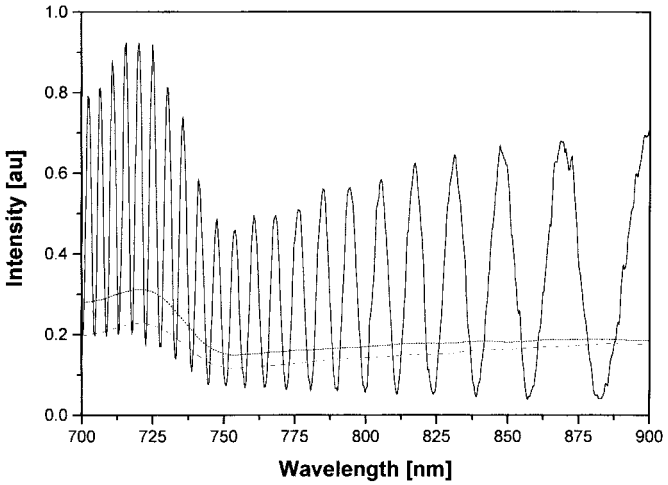

Fig. 3. The smoothed power spectrum of the reference field (dashed) and the signal field (dotted), and the SI signal (solid) for the case where one piece of 0.375″ thick fused silica glass optical flat was placed in thesignal arm of the interferometer.

subtracted them from the interference signal, to account for the nonuniformity of the white light source. The result was transformed to the time-domain by an inverse Fourier transformation, and the negative and zero time terms were filtered out and Fourier transformed back to the frequency-domain. The resulting spectrum was multiplied by a linear phase exponent factor to account for the delay τ, to give the desired spectral phase difference [10]. The spectral phase extracted from the data shown in Fig. 3 is presented as curve (a) in Fig. 4, together with the calculated dispersion curve obtained using the values of $\phi'' = 362$ fs^2/cm and $\phi''' = 275$ fs^3/cm for the second- and third-order dispersion coefficients. These calculated values were obtained using Sellmeir's coefficients for fused silica glass at 800-nm wavelength. Next, we inserted an additional identical optical flat in the signal arm of the

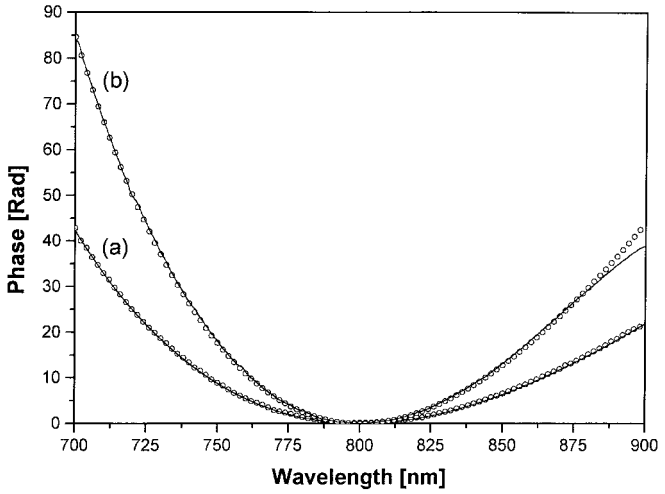

Fig. 4. Extracted (circles) and computed (solid) dispersion for fused silica glass using second- and third-order dispersion coefficients for 800-nm wavelength. (a) One piece of 0.375-in-thick fused silica optical flat. (b) Two pieces of 0.375-in-thick fused silica optical flats.

interferometer. The spectral phase in this case is shown as curve (b) in Fig. 4, together with the calculated dispersion curve, obtained using the same values as above for ϕ'' and ϕ'''. The excellent agreement between the extracted and the calculated data clearly demonstrates the potential of white light SI for dispersion measurements.

Next, we measured dispersion of dielectric coatings. For this purpose, we replaced the silver mirror of the signal arm of the interferometer by various dielectric mirrors. Fig. 5(a) shows the extracted spectral phase for (I) high-reflectance broad-band dielectric mirror, designed for the 450–700-nm wavelengths range, (II) high-reflectance dielectric mirror designed for 1.06-μm wavelength, and (III) 90% output coupler designed for a central wavelength of 800 nm (CVI-PR2 800 90), used for mode-locked Ti:Sapphire lasers. Curves (I) and (II) in Fig. 5(a) show approximately constant spectral phase regions, with abrupt spectral phase jumps between them. The reflectance curves of these dielectric mirrors is shown in Fig. 5(b). It is evident from comparing Fig. 5(a) and (b) that the locations of the phase jumps correspond to minima of the reflectance, where sign reversal of the amplitude reflectance has occurred. These phase distortions could impose severe distortions on short pulses. Curve (III) in Fig. 5(a), which corresponds to a 90% 800-nm output coupler, shows negligible dispersion of the dielectric coating in the relevant spectral range, and smooth reflectance curve, as can be seen in curve (III) in Fig. 5(b). As is well known, dielectric mirrors for femtosecond operation require a linear phase versus frequency over a large bandwidth to minimize dispersion. This is usually achieved by using a single-stack dielectric coating of sufficient bandwidth [17], [18].

Finally, we inserted two 60° SF-18 glass prisms, in a prism-pair arrangement [19], into the signal arm of the interferometer. Fig. 6 shows the extracted dispersion of the prism-pair for three values of beam path-length through the prism glass. The negative second-order dispersion is evident as well as the significant contribution of the third order. From this data,

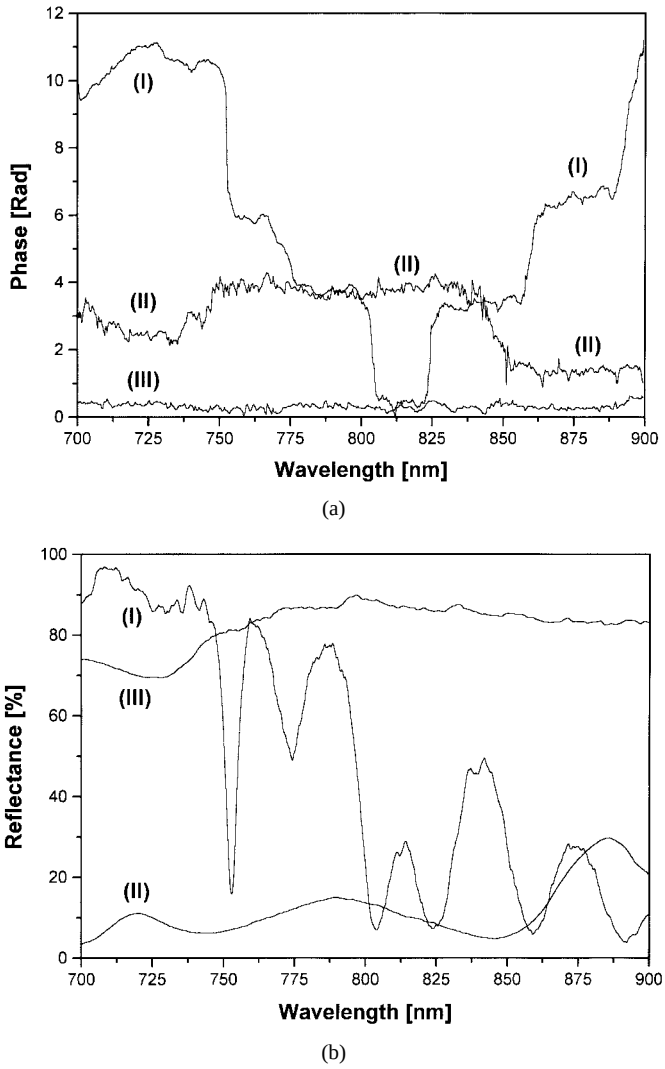

(a)

(b)

Fig. 5. Extracted dispersion and reflectance of dielectric mirrors anddielectric coatings. (a) Dispersion of (I) high-reflectance broad-band dielectric mirror for the 450–700-nm wavelengths range, (II) high-reflectance dielectric mirror for 1060-nm wavelength, and (III) a 90% output coupler designed for a central wavelength of 800 nm (CVI-PR2 800 90), used for mode-locked Ti:Sapphire lasers. (b) The corresponding reflectance curves of the dielectric mirrors (I)–(III).

we extracted dispersion coefficients of $\phi'' = -2160$ fs^2 and $\phi''' = -12\,066$ fs^3 for the short beam path through the prism, $\phi'' = -1172$ fs^2 and $\phi''' = -1152$ fs^3 for the medium beam path and $\phi'' = -1026$ fs^2 and $\phi''' = -12\,330$ fs^3 for the long beam path. It is evident from this data that ϕ'' increases with beam path through the glass, as expected.

B. Spatial-Spectral Interference

The SSI experimental setup is shown in Fig. 2. The white light source for the experiment was an arc Xenon lamp. As in our 1-D SI experiment, the white light source was spatially filtered using the same 5-m-long single-mode optical fiber. The white light was coupled into the optical fiber using a $\times 10$ 0.25 NA microscope objective, and the light emerging from the fiber was collimated using an additional $\times 10$ 0.25 NA microscope objective. As in our previous experiment, the collimated white light beam was split into two by the same

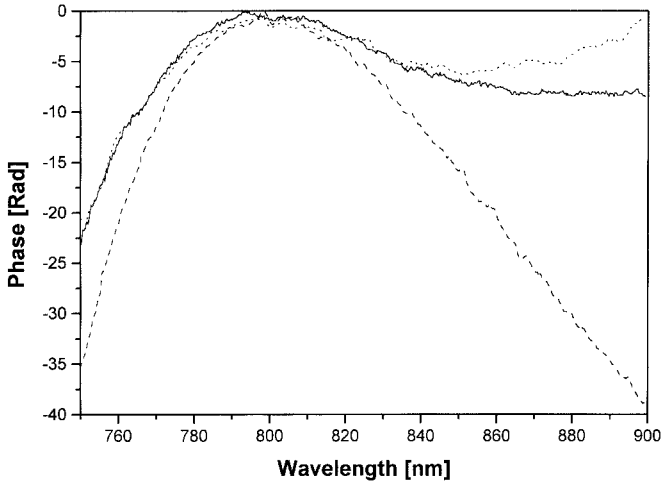

Fig. 6. Extracted dispersion of a 60° SF-18 prism-pair arrangement, for three values of beam path length through the prism glass. The dashed, solid, and dotted curves correspond to short, medium, and long path length in the glass, respectively.

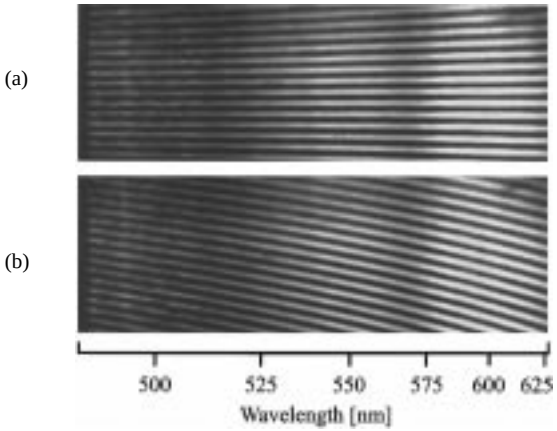

Fig. 7. The SSI pattern of the signal and reference fields, with no spectral phase distortion. (a) No delay. (b) Delay of 67 fs.

broad-band 50/50 dielectric beam splitter for the reference and signal beams. In order to compensate for the residual material dispersion of the interferometer, we inserted additional glass flats into the reference beam (not shown in Fig. 2), to balance the two arms. The signal beam was reflected by a silver mirror, while the reference beam was reflected by a silver mirror corner reflector, adjusted so that the two beams, after having passed again through the beam splitter, propagated at an angle $2\theta = 0.6°$ with respect to each other. The spectral components of the two fields were spatially dispersed by a 60° SF-18 prism, and the spectra of the two beams interfered at the focal plane of a 100-mm focal length cylindrical lens, where a color CCD matrix was placed (COHU 8310). The prism and the cylindrical lens were used to accommodate a bandwidth of 143 nm over the CCD width. At the focal plane, each spectral component was focused down to 50 μm, while the CCD pixel size was $\sim$9 μm. In the following, we describe several measurements of phase distortions that were imposed upon the signal field.

First, we recorded the SSI pattern of the reference and the signal fields, when no distortion was introduced. The results are shown in Fig. 7. The case where the two fields coincide in time is shown in Fig. 7(a). This measurement was also used to confirm that the interferometer was balanced in terms of dispersion, as is evident from the straight lines. Note that the fringe pattern is wedged, due to the fact that the horizontal axis corresponds to wavelength, and therefore the fringe spacing varies. A delay between the two fields corresponds to a linear spectral phase shift, which results in a tilt of the interference pattern. This is clearly seen in Fig. 7(b) where a delay of 67 fs was introduced between the fields [20]. The delay was calculated directly from the fringe pattern, using the definition $\tau(\omega) = [\partial\phi(\omega)/\partial\omega]$. Our calculations based on the fringe pattern gave a delay of 62 fs, a good estimate of the induced delay. Note that the direction of the tilt uniquely determines the temporal relation between the signal and the reference fields, since a negative delay would simply rotate the direction of the fringes. While Fig. 7 shows black and white reproductions, the original image is displayed in colors.[1]

To demonstrate real-time display and measurements of dispersion, we first placed a 3.175-mm-thick fused silica glass optical flat in the signal arm of the interferometer. The interference pattern in this case is shown in Fig. 8(a). The nonlinear mapping of the optical frequencies onto the CCD matrix should be taken into account in interpreting the results. The measurements yield a quadratic dispersion coefficient of $\phi'' = 652$ fs^2/cm for the fused silica glass, for a central wavelength of 555 nm. This is in good agreement with the calculated value of 621 fs^2/cm, obtained using Sellmeir's coefficients for fused silica glass for this wavelength. The sign of the dispersion is clearly reflected from the curvature of the fringes. Placing the optical flat in the reference beam resulted with an inverted interference pattern. Next, we replaced the optical glass flat in the signal arm of the interferometer by a 9.525-mm fused silica glass optical flat. The resulting interference pattern is shown in Fig. 8(b). The measurements yield a quadratic dispersion coefficient of $\phi'' = 634$ fs^2/cm, which is in excellent agreement with the calculated value.

We have also used SSI for real-time dispersion measurements of dielectric mirrors. To demonstrate this, we replaced the silver mirror of the signal arm of the interferometer by various dielectric mirrors. Fig. 9(a) shows the interference pattern when the silver mirror of the signal arm was replaced by a high-reflectance broad-band dielectric mirror, designed for the 450–700-nm wavelengths. The variation of the spectral interference fringes, shown in Fig. 9(a), reveals a spectral phase distortion across the spectrum. Since the mirror is designed for high reflectance over the measurement range, we attribute the phase structure to the existence of several reflectance stacks in the dielectric coating. Finally, we replaced this mirror by a dielectric mirror, designed for the 1060-nm wavelength. The resulting interference pattern is shown in Fig. 9(b). Here it is evident that the spectral phase jumps occur at wavelengths where low reflectance is observed, corresponding

[1]The original colored version of the SSI images presented in this paper can be viewed at our home page, http://www.weizmann.ac.il/physics/complex/ultrafast.

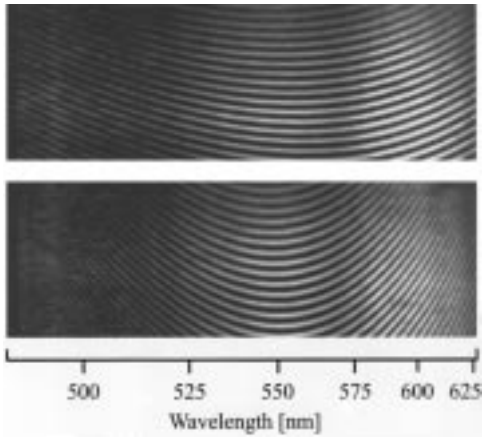

Fig. 8. The SSI pattern of the signal and the reference fields, when optical glasses were inserted in the signal arm. (a) 3.175 mm of fused silica optical glass. (b) 9.525 mm of fused silica optical glass.

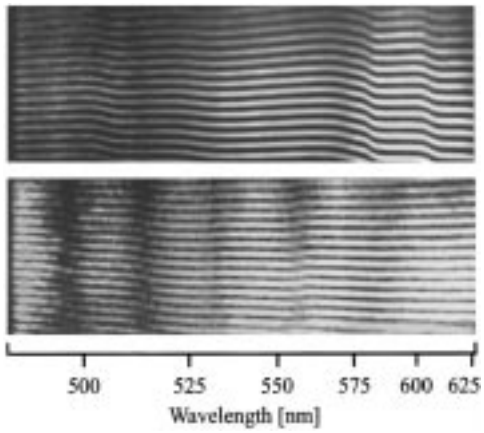

Fig. 9. The SSI pattern of the signal and the reference fields, when the silver mirror of the signal arm of the interferometer was replaced by dielectric mirrors. (a) High-reflectance broad-band dielectric mirror for the 450–700-nm wavelengths. (b) High-reflectance dielectric mirror for the 1060-nm wavelength.

to phase reversal in the amplitude reflectance sidelobes, as discussed previously for the method of SI.

IV. Conclusion

One- and two-dimensional white light SI techniques were demonstrated for the measurement of dispersion of optical glasses, dielectric coatings, and prism-pair arrangements. The techniques of white light SI and SSI involve a linear detection, and therefore weak fields can be measured. The technique of white light SI was shown useful for accurate dispersion measurements over a wide bandwidth, however, post-processing and unwrapping of the spectral phase is needed. White light SSI removes these difficulties. No scanning or motion is involved, so that fast measurements are possible. Finally, we would like to note that SSI could be used for dynamic real-time material dispersion measurements, and therefore it is very convenient for alignment of optical setups to eliminate dispersion or to bring it to a required value.

References

[1] C. Spielmann, P. F. Curley, T. Brabec, and F. Krausz, "Ultrabroadband femtosecond lasers," *IEEE J. Quantum Electron.*, vol. 30, pp. 1100–1114, 1994.
[2] A. Baltuska, Z. Wei, M. S. Pshenichnikov, and D. A. Wiersma, "Optical pulse compression to 5 fs at a 1-MHz repetition rate," *Opt. Lett.*, vol. 22, pp. 102–104, 1997.
[3] A. A. Michelson, *Light Waves and Their Uses*. Chicago, IL: Chicago Press, 1902.
[4] W. H. Knox, N. M. Pearson, K. D. Li, and C. A. Hirlimann, "Interferometric measurements of femtosecond group delay in optical components," *Opt. Lett.*, vol. 13, pp. 574–576, 1988.
[5] W. H. Knox, "Dispersion measurements for femtosecond-pulse generation and applications," *Appl. Phys. B*, vol. 58, pp. 225–235, 1994.
[6] M. Tateda, N. Shibata, and S. Seikai, "Interferometric method for chromatic dispersion measurement in a single-mode optical fiber," *IEEE J. Quantum Electron.*, vol. QE-17, pp. 404–407, 1981.
[7] J. Stone and L. G. Cohen, "Minimum-dispersion spectra of single-mode fibers measured with subpicosecond resolution by white-light crosscorrelation," *Electron. Lett.*, vol. 18, pp. 716–718, 1982.
[8] M. Beck and I. A. Walmsley, "Measurement of group delay with high temporal and spectral resolution," *Opt. Lett.*, vol. 15, pp. 492–494, 1990.
[9] M. Beck, I. A. Walmsley, and J. D. Kafka, "Group delay measurements of optical components near 800 nm," *IEEE J. Quantum Electron.*, vol. 27, pp. 2074–2081, 1991.
[10] D. N. Fittinghoff, J. L. Bowie, J. N. Sweetser, R. T. Jennings, M. A. Krumbügel, K. W. DeLong, R. Trebino, and I. A. Walmsley, "Measurement of the intensity and phase of ultraweak, ultrashort laser pulses," *Opt. Lett.*, vol. 21, pp. 884–886, 1996.
[11] C. Froehly, A. Lacourt, and J. C. Viénot, "Time impulse response and time frequency response of optical pupils. Experimental confirmations and applications," *J. Opt.*, vol. 4, pp. 183–196, 1973.
[12] L. Lepetit, G. Chériaux, and M. Joffre, "Linear techniques of phase measurement by femtosecond spectral interferometry for applications in spectroscopy," *J. Opt. Soc. Amer., B*, vol. 12, pp. 2467–2474, 1995.
[13] J. Piasecki, B. Colombeau, M. Vampouille, C. Froehly, and J. A. Arnaud, "Nouvelle méthode de mesure de la réponse impulsionnelle des fibers optiques," *Appl. Opt.*, vol. 19, pp. 3749–3755, 1980.
[14] A. P. Kovács, K. Osvay, Zs. Bor, and R. Szipöcs, "Group-delay measurement on laser mirrors by spectrally resolved white-light interferometry," *Opt. Lett.*, vol. 20, pp. 788–790, 1995.
[15] K. Misawa and T. Kobayashi, "Femtosecond Sagnac interferometer for phase spectroscopy," *Opt. Lett.*, vol. 20, pp. 1550–1552, 1995.
[16] D. Meshulach, D. Yelin, and Y. Silberberg, "Real-time spatial-spectral interference measurements of ultrashort optical pulses," *J. Opt. Soc. Amer. B*, vol. 14, pp. 2095–2098, 1997.
[17] S. De Silvestri, P. Laporta, and O. Sveldo, "Analysis of quarter-wave dielectric-mirror dispersion in femtosecond dye-laser cavities," *Opt. Lett.*, vol. 9, pp. 335–337, 1984.
[18] A. M. Weiner, J. G. Fujimoto, and E. P. Ippen, "Femtosecond time-resolved reflectomery measurements of multiple-layer dielectric mirrors," *Opt. Lett.*, vol. 10, pp. 71–73, 1985.
[19] R. L. Fork, O. E. Martinez, and J. P. Gordon, "Negative dispersion using pairs of prisms," *Opt. Lett.*, vol. 9, pp. 150–152, 1984.
[20] A. M. Weiner, D. E. Leaird, D. H. Reitze, and E. G. Paek, "Femtosecond spectral holography," *IEEE J. Quantum Electron.*, vol. 28, pp. 2251–2261, 1992.

D. Meshulack, photograph and biography not available at the time of publication.

D. Yelin, photograph and biography not available at the time of publication.

Y. Silberlberg, photograph and biography not available at the time of publication.